Bioorganic & Medicinal Chemistry Letters 26 (2016) 924–927

Contents lists available at ScienceDirect

Bioorganic & Medicinal Chemistry Letters

journal homepage: www.elsevier.com/locate/bmcl

Design, radiosynthesis, and evaluation of radiotracers for positron emission tomography imaging of stearoyl-CoA desaturase-1

William C. Silvers [a], Hancheng Cai [a,b], Orhan K. Öz [a], Xiankai Sun [a,b,*]

[a] Department of Radiology, The University of Texas Southwestern Medical Center, Dallas, TX 75390, USA
[b] Advanced Imaging Research Center, The University of Texas Southwestern Medical Center, Dallas, TX 75390, USA

ARTICLE INFO

Article history:
Received 11 December 2015
Revised 17 December 2015
Accepted 18 December 2015
Available online 19 December 2015

Keywords:
Stearoyl-CoA desaturase
De novo lipid metabolism
Radiosynthesis
PET
^{18}F-FPPPT

ABSTRACT

Design, radiosynthesis, and biological evaluation of two radiotracers (*N*-(3-[^{18}F]fluoropropyl)-6-(4-(trifluoromethyl)benzoyl)-piperazin-1-yl)pyridazine-3-carboxamide (^{18}F-FPPPT) and (*N*-(4-[^{18}F]fluoroaniline)-6-(4-(trifluoromethyl)benzoyl)-piperazin-1-yl)pyridazine-3-carboxamide (^{18}F-FAPPT)) are described for noninvasive assessment of stearoyl-CoA desaturase-1 (SCD-1). The overexpression of SCD-1 in multiple solid tumors associates with poor survival in cancer patients. The two radiotracers, ^{18}F-FPPPT and ^{18}F-FAPPT, were each prepared in three steps in radiochemical yields of 21% and 3%, respectively. The practicality of imaging SCD-1 with ^{18}F-FPPPT was tested in two mouse models bearing xenograft tumors with different levels of SCD-1 expression, which afforded a 1.8-fold uptake difference correspondingly. Our work indicates that it is possible to develop SCD-1 specific imaging probes from previously reported SCD-1 inhibitors.

The family of stearoyl-CoA desaturase (SCD) enzymes catalyzes the formation of a double bond at the C9 position in saturated fatty acids (SFAs) to create monounsaturated fatty acids (MUFAs).[1–3] Of the two isoforms in humans, SCD-1 is predominant and ubiquitously expressed in the brain, liver, fat, heart and lung.[4] Upregulated expression of SCD-1 has been reported in multiple solid tumors (e.g., prostate, breast, lung, and ovarian cancer) with implications in cancer progression, which is indicative of poor prognosis in cancer patients.[5,6] The important role of SCD-1 in *de novo* fatty acid (FA) metabolism, a pathway elevated across all cancer types, makes it an ideal target for cancer therapy. To date, small organic inhibitors of SCD-1 have shown desired anti-cancer effects by inducing cancer cell apoptosis and slowing tumor-growth in preclinical tumor xenograft mouse models.[6–8] Given the reported correlation of SCD-1 expression with cancer progression, measurement of SCD-1 levels can potentially serve as a biomarker for cancer treatment planning and prognostic evaluation post-treatment.

Clinically, the expression of SCD-1 is often measured by the desaturation index (DI) from plasma and tissue or immunohistochemical analysis on tissue biopsies.[5,9,10] Suboptimal accuracy of biopsies aside, major drawbacks of both methods include the invasiveness of obtaining biopsies from tissues and long sample processing times. A noninvasive imaging technique would be highly desirable in the clinic for the assessment of SCD-1 expression.

To date, numerous SCD-1 inhibitors with sub-μM binding affinities have been reported for cancer treatment.[11–15] These inhibitors can potentially serve as lead compounds for SCD-1 targeted radiotracer development.

To enable positron emission tomography (PET) imaging of SCD-1, the design of radiotracers labeled with ^{18}F ($t_{1/2}$ = 109.8 minutes; β^+ 0.63 MeV, 97%) was based on two previously reported SCD-1 inhibitors, *N*-pentyl-6-(4-(2-(trifluoromethyl)benzoyl)piperazin-1-yl)pyrazine-3-carboxamide and *N*-phenethyl-6-(4-(2-(trifluoromethyl)benzoyl)piperazin-1-yl)pyrazine-3-carboxamide.[15] Their half maximal inhibitory concentrations (IC_{50}) were measured at 25 and 18 nM, respectively, for human SCD-1. Shown in Scheme 1, the ^{18}F synthon (**1**) for ^{18}F-FAPPT (*N*-(4-[^{18}F]fluoroaniline)-6-(4-(trifluoromethyl)benzoyl)-piperazin-1-yl)pyridazine-3-carboxamide) was synthesized as previously described.[16] To make the synthon (**5**) for ^{18}F-FPPPT (*N*-(3-[^{18}F]fluoropropyl)-6-(4-(trifluoromethyl) benzoyl)-piperazin-1-yl)pyridazine-3-carboxamide), the desired tosylated precursor (**3**) was first prepared through reacting *N*-(*tert*-butoxycarbonyl)-3-hydroxypropylamine (**2**)[17] with *p*-toluenesulfonyl chloride in the presence of triethylamine (Et_3N) (63% yield).[18] Synthesis of ^{18}F-FPPPT was accomplished in 3 steps within 120 min, as outlined in Scheme 1.[19] Radiolabeling of **3** with ^{18}F was performed under basic conditions in the presence of kryptofix 2,2,2 ($K_{2,2,2}$)/K_2CO_3 and the reaction was carried out at 110 °C for 15 min. The resulting protected 3-[^{18}F]fluoro-propylamine **4** was isolated

* Corresponding author.

http://dx.doi.org/10.1016/j.bmcl.2015.12.062
0960-894X/

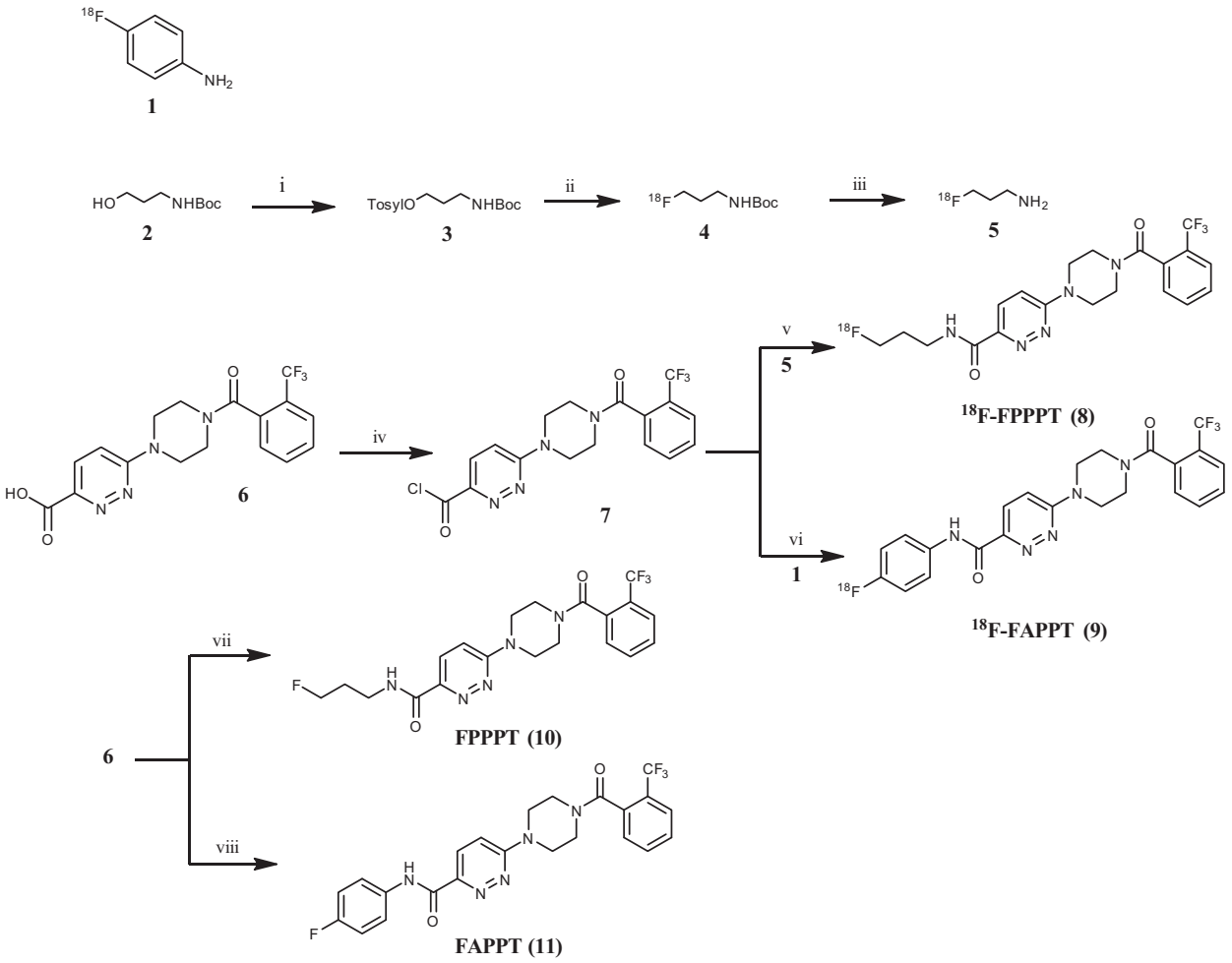

Scheme 1. Synthesis of ^{18}F-FPPPT, ^{18}F-FAPPT, synthons **1** and **5**, FPPPT, and FAPPT. Reagents and conditions: (i) *p*-toluenesulfonyl chloride, DMAP, Et_3N, dichloromethane (DCM); (ii) $K_{2.2.2}/K_2CO_3$, acetonitrile (ACN), 110 °C, 15 min; (iii) TFA, rt, 8 min; (iv) thionyl chloride, DCM, 50 °C, overnight; (v) **5**, Et_3N, ACN, rt, 15 min; (vi) **1**, Et_3N, ACN, rt, 15 min; (vii) 3-fluoropropylamine hydrochloride, HBTU, DIPA, dimethylformamide (DMF); (viii) 4-fluoroanline, HBTU, DIPEA, DMF.

on a C-18 Sep-Pak cartridge, which was eluted into a vial and dried under a nitrogen flow. Compound **4** was then deprotected by trifluoroacetic acid (TFA, neat) for 8 min generating ^{18}F-fluoro-propylamine (**5**) in 51% radiochemical yield (RCY). After removal of TFA, the silica Sep-Pak cartridge trapped **5** was eluted with acetonitrile for further radiochemistry. For the synthesis of ^{18}F-FPPPT and ^{18}F-FAPPT, 6-(4-(2-(trifluoromethyl)benzoyl)piperazine-1-yl)-pyridazine-3-carboxylate (**6**) was prepared according to a published procedure, from which the amine reactive acid chloride analog **7** was obtained by reacting with thionyl chloride. Compound **7** is the common precursor to make both ^{18}F-FPPPT and ^{18}F-FAPPT by reacting with synthons **5** and **1**, respectively.[20] The coupling reaction between **5** and **7** was carried out at room temperature (rt) for 15 min, followed by HPLC purification of ^{18}F-FPPPT on a semi-preparative C-18 column. The decay corrected RCY at the end of synthesis (EOS) was 21%. The radiochemical purity of the obtained ^{18}F-FPPPT was 99%. The synthesis of ^{18}F-FAPPT was accomplished in a similar way by reacting **1** with **7**.[21] The decay corrected RCY of ^{18}F-FAPPT was lower at 3% at the EOS, due to the poor reactivity of aromatic amines as opposed to the aliphatic in ^{18}F-FPPPT synthesis, and its radiochemical purity was 99%. The average ($n = 3$) specific radioactivity for ^{18}F-FPPPT and ^{18}F-FAPPT was 507 ± 148 MBq μmol^{-1} and 61 ± 28 MBq μmol^{-1}, respectively. The reference standard compounds, the ^{19}F counterparts of ^{18}F-FPPPT and ^{18}F-FAPPT, were synthesized by reacting **6** with 3-fluoropropylamine or 4-fluoroaniline in the presence of *N*,*N*-diisopropylethylamine (DIPEA) using *O*-(benzotriazo-1-yl)-*N*,*N*,*N*′*N*′-tetramethyluronium hexafluorophosphate (HBTU) as the coupling agent at yields of 85% and 80%, respectively, as shown in Scheme 1.[22,23]

The lipophilicity of ^{18}F-FPPPT and ^{18}F-FAPPT measured by partition coefficient (log*P*) was assessed in a bi-phasic mixture of *n*-octanol and water.[24] The log*P* values of ^{18}F-FPPPT and ^{18}F-FAPPT were determined to be 1.23 and 2.08, respectively. The lipophilicity difference of ^{18}F-FPPPT and ^{18}F-FAPPT can be attributed to the fact that different linkers, phenyl and propyl, were used for their construction. The stability of ^{18}F-FPPPT and ^{18}F-FAPPT in fetal bovine serum (FBS) was assessed by radio-HPLC after 3 h of incubation at 37 °C. Both radiotracers were found nearly 100% intact.

The SCD-1 mediated retention of ^{18}F-FPPPT and ^{18}F-FAPPT was assayed in SCD-1 positive prostate cancer cells (C4-2; Fig. 1a) with a commercially available SCD-1 inhibitor, 4-(2-chlorophenoxy)-*N*-[3-[(methylamino)carbonyl]phenyl]-1-piperidinecarboxamide (IC_{50} = 37 nM for human SCD-1) (Fig. 1b).[25,26] Briefly, ~2.0 μCi of each radiotracer was incubated with or without the inhibitor in C4-2 cells for 30 min, followed by rinsing with fresh media to remove non-specifically bound radiotracer. The cells were later trypsinized and the activity was measured and normalized to the cell numbers. Shown in Figure 1b, the SCD-1 mediated C4-2 cell uptake reduced by 40% and 39% for ^{18}F-FPPPT and ^{18}F-FAPPT,

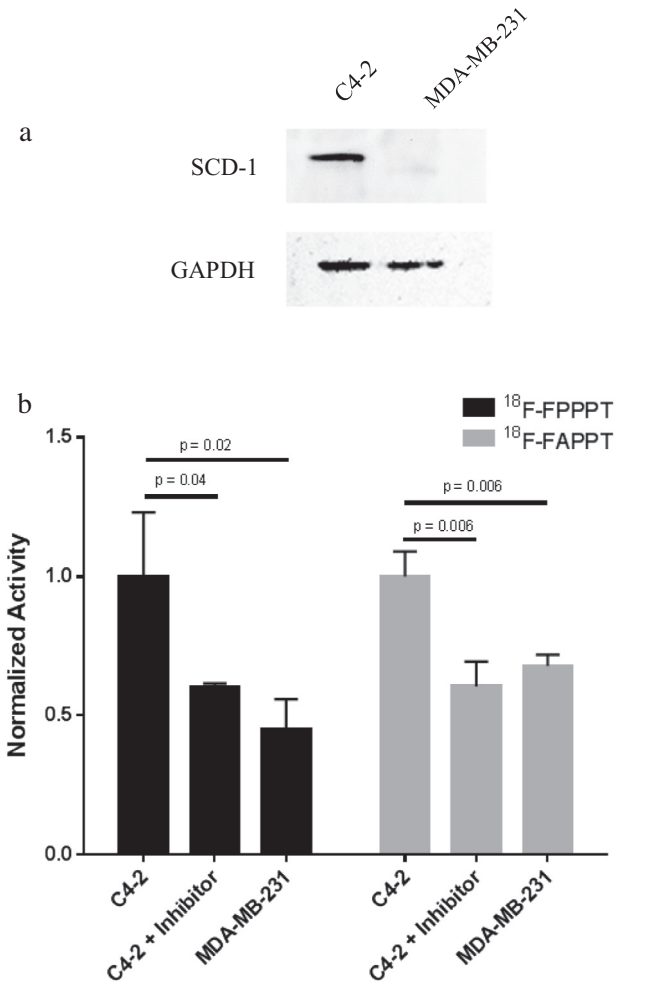

Figure 1. In vitro evaluation of ^{18}F-FPPPT and ^{18}F-FAPPT in cancer cells. (a) Western blot showing protein expression of SCD-1 in C4-2 and MDA-MB-231 cells with GAPDH as loading control. (b) SCD-1 mediated retention of ^{18}F-FPPPT and ^{18}F-FAPPT in C4-2 cells with and without co-incubation of an SCD-1 inhibitor and MDA-MB-231 cells.

respectively, by the blockade with the inhibitor, which indicates the specific binding of the radiotracers to SCD-1. Further, ^{18}F-FPPPT and ^{18}F-FAPPT showed 2.2-fold and 1.5-fold higher uptake, respectively, in C4-2 cells than in a low SCD-1 expressing MDA-MB-231 cell line (Fig. 1a).

Given its higher SCD-1 specific uptake, ^{18}F-FPPPT was selected to test the feasibility of imaging SCD-1 in vivo in mouse models bearing tumor xenografts with high (PC-3) and low (MDA-MB-231) SCD-1 expression as determined by western blot (Fig. 2a). Each mouse was injected with ~100 μCi and underwent PET imaging at 1 h post-injection (p.i.).[27] As shown in Figure 2b, the tumor with high SCD-1 expression, PC-3, was clearly visualized, while the one with low SCD-1 expression, MDA-MB-231, showed an uptake level barely above the background. Further quantitative analysis revealed that the uptake of ^{18}F-FPPPT in the PC-3 tumor was 1.8-fold higher than in the MDA-MB-231 tumor, which is consistent with the in vitro result presented in Figure 1. Of note, high bone uptake was observed in the scans of both animal models, likely due to defluorination of ^{18}F from the alkyl subunit. Other ^{18}F-labeled synthons with higher stability will be employed to minimize or overcome the problem of defluorination in future.

In summary, we have successfully synthesized two PET radiotracers (^{18}F-FPPPT and ^{18}FPPPT) for noninvasive imaging of SCD-1. The synthesis of each radiotracer was achieved with low to high

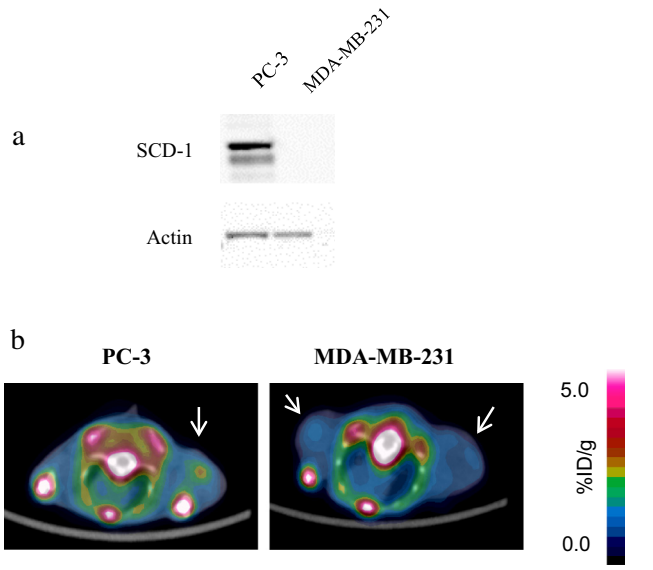

Figure 2. (a) Western blot showing protein expression of SCD-1 in PC-3 and MDA-MB-231 cells with actin as loading control. (b) Transaxial PET images of PC-3 and MDA-MB-231 tumors with ^{18}F-FPPPT in NOD-SCID mice (1 h p.i.). Tumors marked with white arrows.

RCY with high specific radioactivity and radiochemical purity. Both radiotracers were found to exhibit SCD-1 mediated retention in SCD-1 expressing prostate cancer cells in vitro, with ^{18}F-FPPPT having higher specific retention. In vivo evaluation in mouse xenograft models demonstrated the ability of PET with ^{18}F-FPPPT to differentiate tumors with high and low SCD-1 expression.

Acknowledgments

This study was partially supported by a grant from the National Institutes of Health (R01 DK092163) and the Dr. Jack Krohmer Professorship Funds. The Professorship Funds is an endowment provided to the corresponding author by University of Texas Southwestern Medical Center.

Supplementary data

Supplementary data associated with this article can be found, in the online version, at http://dx.doi.org/10.1016/j.bmcl.2015.12.062.

References and notes

1. Paton, C. M.; Ntambi, J. M. *Am. J. Physiol. Endocrinol. Metab.* **2009**, *297*, E28.
2. Ntambi, J. M.; Miyazaki, M.; Stoehr, J. P.; Lan, H.; Kendziorski, C. M.; Yandell, B. S.; Song, Y.; Cohen, P.; Friedman, J. M.; Attie, A. D. *Proc. Natl. Acad. Sci. U.S.A.* **2002**, *99*, 11482.
3. Ntambi, J. M.; Miyazaki, M.; Dobrzyn, A. *Lipids* **2004**, 39.
4. Zhang, L.; Ge, L.; Parimoo, S.; Stenn, K.; Prouty, S. M. *Biochem. J.* **1999**, *340*, 255.
5. Holder, A. M.; Gonzalez-Angulo, A. M.; Chen, H.; Akcakanat, A.; Do, K. A.; Fraser Symmans, W.; Pusztai, L.; Hortobagyi, G. N.; Mills, G. B.; Meric-Bernstam, F. *Breast Cancer Res. Treat.* **2013**, *137*, 319.
6. Roongta, U. V.; Pabalan, J. G.; Wang, X.; Ryseck, R.-P.; Fargnoli, J.; Henley, B. J.; Yang, W.-P.; Zhu, J.; Madireddi, M. T.; Lawrence, R. M.; Wong, T. W.; Rupnow, B. A. *Mol. Cancer Res.* **2011**, *9*, 1551.
7. Fritz, V.; Benfodda, Z.; Rodier, G.; Henriquet, C.; Iborra, F.; Avancès, C.; Allory, Y.; de la Taille, A.; Culine, S.; Blancou, H.; Cristol, J. P.; Michel, F.; Sardet, C.; Fajas, L. *Mol. Cancer Ther.* **2010**, *9*, 1740.
8. von Roemeling, C. A.; Marlow, L. A.; Wei, J. J.; Cooper, S. J.; Caulfield, T. R.; Wu, K.; Tan, W. W.; Tun, H. W.; Copland, J. A. *Clin. Cancer Res.* **2013**, *19*, 2368.
9. Jeyakumar, S. M.; Lopamudra, P.; Padmini, S.; Balakrishna, N.; Giridharan, N. V.; Vajreswari, A. *Nutr. Metab. (Lond.)* **2009**, *6*, 1.
10. Ide, Y.; Waki, M.; Hayasaka, T.; Nishio, T.; Morita, Y.; Tanaka, H.; Sasaki, T.; Koizumi, K.; Matsunuma, R.; Hosokawa, Y.; Ogura, H.; Shiiya, N.; Setou, M. *PLoS ONE* **2013**, *8*, e61204.

11. Isabel, E.; Powell, D. A.; Black, W. C.; Chan, C.-C.; Crane, S.; Gordon, R.; Guay, J.; Guiral, S.; Huang, Z.; Robichaud, J.; Skorey, K.; Tawa, P.; Xu, L.; Zhang, L.; Oballa, R. *Bioorg. Med. Chem. Lett.* **2011**, *21*, 479.
12. Yang, S.-M.; Tang, Y.; Rano, T.; Lu, H.; Kuo, G.-H.; Gaul, M. D.; Li, Y.; Ho, G.; Lang, W.; Conway, J. G.; Liang, Y.; Lenhard, J. M.; Demarest, K. T.; Murray, W. V. *Bioorg. Med. Chem. Lett.* **2014**, *24*, 1437.
13. Powell, D. A.; Black, W. C.; Bleasby, K.; Chan, C.-C.; Deschenes, D.; Gagnon, M.; Gordon, R.; Guay, J.; Guiral, S.; Hafey, M. J.; Huang, Z.; Isabel, E.; Leblanc, Y.; Styhler, A.; Xu, L.-J.; Zhang, L.; Oballa, R. M. *Bioorg. Med. Chem. Lett.* **2011**, *21*, 7281.
14. Deng, Y.; Yang, Z.; Shipps, G. W., Jr.; Lo, S.-M.; West, R.; Hwa, J.; Zheng, S.; Farley, C.; Lachowicz, J.; van Heek, M.; Bass, A. S.; Sinha, D. P.; Mahon, C. R.; Cartwright, M. E. *Bioorg. Med. Chem. Lett.* **2013**, *23*, 791.
15. Zhang, Z.; Sun, S.; Kodumuru, V.; Hou, D.; Liu, S.; Chakka, N.; Sviridov, S.; Chowdhury, S.; McLaren, D. G.; Ratkay, L. G.; Khakh, K.; Cheng, X.; Gschwend, H. W.; Kamboj, R.; Fu, J.; Winther, M. D. *J. Med. Chem.* **2013**, *56*, 568.
16. Monaco, A.; Zoete, V.; Alghisi, G. C.; Rüegg, C.; Michelin, O.; Prior, J.; Scapozza, L.; Seimbille, Y. *Bioorg. Med. Chem. Lett.* **2013**, *23*, 6068.
17. Hung, A. H.; Holbrook, R. J.; Rotz, M. W.; Glasscock, C. J.; Mansukhani, N. D.; MacRenaris, K. W.; Manus, L. M.; Duch, M. C.; Dam, K. T.; Hersam, M. C.; Meade, T. J. *ACS Nano* **2014**, *8*, 10168.
18. *Synthesis of* **3**: *N*-(*tert*-butoxycarbonyl)-3-hydroxypropylamine (2.4 g, 13.7 mmol) was dissolved in 60 mL DCM under nitrogen. To the reaction was added 2.23 mL (16 mmol) Et_3N, followed by 3.12 g (16.4 mmol) *p*-toluenesulfonyl chloride and 100 mg DMAP in 20 mL DCM. The reaction was stirred overnight and solvent removed. The reaction was purified on a silica column with a mobile phase of 2:1 Hexanes/EtOAc. The product was dried under high vacuum, giving 2.82 g (63% yield) of a colorless solid. ^{1}H NMR (400 MHz, $CDCl_3$) δ 7.80 (d, 2H), 7.37 (d, 2H), 4.09 (t, 2H), 3.17 (d, 2H), 2.45 (s, 3H), 1.86 (q, 2H) 1.42 (s, 9H). *m*/*z* (ESI-TOF): 174.11 $[M+H]^+$, calcd 174.14.
19. *Radiosynthesis of* ^{18}*F-FPPPT* (**8**): Radiosynthesis of **4** was carried out in a GE FXN module. Approximately 7.0 mg of **3** in 0.7 mL dry ACN was added to dried ^{18}F in 1.0 mg $K_{2.2.2}$ and 1.0 mg K_2CO_3 and the reaction mixture was heated for 15 min at 110 °C. After cooling to rt, the crude mixture was diluted with 10 mL water and flushed through a C-18 Sep-Pak cartridge, trapping the Boc protected 3-[^{18}F] fluoro-propylamine **4**. The product was eluted with 1.5 mL ACN into a reaction vial and dried by heating to 70 °C and flowing nitrogen. When dry, the product was Boc deprotected by adding 0.8 mL TFA (neat). After 8 min at rt the reaction was diluted with 20 mL DCM and flushed through a silica Sep-Pak cartridge trapping **5**. The product was eluted with 1.5 mL ACN into a round bottom flask with a stir bar and dried by heating to 70 °C and flowing nitrogen. Approximately 20 mg of **7** in 1.0 mL ACN was added to the flask followed with 200 μL Et_3N. After 15 min, the reaction was diluted with 3.0 mL water and the reaction was purified with a semi-preparative RP-HPLC (Phenomenex C18, 10 × 250 mm) and a mobile phase of 40% ACN in water containing 0.01% TFA at a flow rate of 4 mL/min. The fractions containing the product (retention time of 14–16 min.) based on γ-detector were collected, diluted to 50 mL with water, and passed through a C-18 Sep-Pak cartridge to trap ^{18}F-FPPPT. ^{18}F-FPPPT was eluted with 1.5 mL of 85% absolute ethanol in saline. Radiochemical purity was determined by analyzing the portion of the eluent with an analytical RP-HPLC column.
20. *Synthesis of* **7**: Approximately 20 mg (0.05 mmol) of **6** was dissolved in 2 mL dry chloroform in a round bottom flask and heated to 50 °C. To the flask was added 2 drops of DMF and 150 μL thionyl chloride and the solution was left to stir overnight. Solvent was removed with flowing nitrogen and the flask was placed under high vacuum to dry. Compound **7** was used without purification.
21. *Radiosynthesis of* ^{18}*F-FAPPT* (**9**): Synthesis of **1** was carried out in a GE FXN module under conditions previously described.[18] After synthesis, **1** (in methanol) was added to a round bottom flask and dried with flowing nitrogen and heating to 70 °C. Approximately 20 mg of **7** in 1.0 mL ACN was added to the flask followed with 200 μL Et_3N. After 15 min., the reaction was diluted with 3.0 mL water and purified using a semi preparative RP-HPLC (Phenomenex C18, 10 × 250 mm) and a mobile phase of 50% ACN in water containing 0.01% TFA at a flow rate of 4 mL/min. The fractions containing the product (retention time of 16–18 min.) based on γ-detector were collected, diluted to 50 mL with water, and passed through a C-18 Sep-Pak cartridge to trap ^{18}F-FAPPT. ^{18}F-FAPPT was eluted with 1.5 mL of 85% absolute ethanol in saline. Radiochemical purity was determined by analyzing the portion of the eluent with an analytical RP-HPLC column.
22. *Synthesis of FPPPT* (**10**): 6-(4-(2-(trifluoromethyl)benzoyl)piperazine-1-yl)-pyridazine-3-carboxylate (200 mg, 0.53 mmol) and 92 mg (0.81 mmol) 3-fluoropropylamine hydrochloride were dissolved in 4 mL DMF under nitrogen. To the reaction was added 301 mg (0.79 mmol) HBTU, followed by 113 μL DIPEA. The reaction was left to stir overnight and the solvent was removed under vacuum. The reaction was purified using a silica column with a mobile phase of 5% MeOH in EtOAc. Fractions containing the product were collected and solvent was removed. The product was dried under high vacuum, yielding 197 mg (85% yield) of a colorless solid. *m*/*z* (ESI-TOF): 440.19 $[M+H]^+$, calcd 440.17.
23. *Synthesis of FAPPT* (**11**): 6-(4-(2-(trifluoromethyl)benzoyl)piperazine-1-yl)-pyridazine-3-carboxylate (30 mg, 0.079 mmol) and 11.3 mg (0.1 mmol) 4-fluoroanline were dissolved in 2 mL DMF under nitrogen. To the reaction was added 29 mg (0.1 mmol) HBTU, followed by 27.5 DIPEA. The reaction was left to stir overnight and the solvent was removed under vacuum. The reaction was purified on a silica column with a mobile phase of 2:1 EtOAc/hexanes. Fractions containing the product were collected and solvent removed. The product was dried under high vacuum yielding 197 mg (85% yield) of a colorless solid. *m*/*z* (ESI-TOF): 474.04 $[M+H]^+$, calcd 474.05.
24. *Determination of the partition coefficient (log P):* 10 μL of ^{18}F-FPPPT was added to a solution containing 0.5 mL of Milli-Q water and 0.5 mL of *n*-octanol. The sample vials were vortexed for 1 min at rt and allowed to sit for 30 min to allow complete separation of phases. Aliquots of 100 μL from each phase were removed and activity counted separately by a Perkin–Elmer γ-counter. The partition coefficient was calculated as the ratio of counts in the octanol fraction to the counts in the water fraction. Each log *P* determination was performed in triplicate. .
25. *Western blot analysis:* Cell lysates were separated on a 4–12% Bis–Tris (NuPAGE) gel and transferred to a nitrocellulose membranes using an iBlot (Thermo Fisher Scientific) transfer system. Membranes were blocked with 5% milk in TBST for 1 hour and incubated overnight with the appropriate primary antibody. After washing the membrane, it was incubated with the secondary HRP-conjugated antibody, and developed with Supersignal West Pico ECL substrate (Thermo Fisher Scientific). The following antibodies were used: anti-SCD-1 (abcam, ab19862) and anti-Actin (abcam, ab3280), anti-GAPDH (ab181602), HRP donkey anti-rabbit (ab6802) and HRP donkey anti-mouse (ab6820).
26. Xin, Z.; Zhao, H.; Serby, M. D.; Liu, B.; Liu, M.; Szczepankiewicz, B. G.; Nelson, L. T. J.; Smith, H. T.; Suhar, T. S.; Janis, R. S.; Cao, N.; Camp, H. S.; Collins, C. A.; Sham, H. L.; Surowy, T. K.; Liu, G. *Bioorg. Med. Chem. Lett.* **2008**, *18*, 4298.
27. *PET/CT imaging procedures:* PET/CT imaging was performed on a small animal Siemens Inveon PET/CT imaging system. Approximately 100 μCi of ^{18}F-FPPPT in saline was injected through the tail vein into NOD-SCID mice bearing subcutaneous PC-3 or MDA-MB-231 tumors on the front shoulder. Each mouse underwent a static scan 1.0 h p.i.